Atmos. Chem. Phys. Discuss., 9, 9267–9290, 2009
www.atmos-chem-phys-discuss.net/9/9267/2009/

Atmospheric Chemistry and Physics Discussions

This discussion paper is/has been under review for the journal *Atmospheric Chemistry and Physics (ACP)*. Please refer to the corresponding final paper in *ACP* if available.

$H_2{}^{16}O$ and HDO measurements with IASI/MetOp

H. Herbin[1,*], D. Hurtmans[1], C. Clerbaux[1,2], L. Clarisse[1,], and P.-F. Coheur[1,**]**

[1]Spectroscopie de l'Atmosphère, Service de Chimie Quantique et de Photophysique, Université Libre de Bruxelles, Brussels, Belgium
[2]UPMC Université Paris 06, CNRS UMR8190, LAT-MOS/IPSL, Paris, France
[*]now at: Laboratoire d'Optique Atmosphérique, Université des Sciences et Technologies de Lille, 59655 Villeneuve d'Ascq cedex, France
[**]They are Research Associate and Scientific Research Worker with the F.N.R.S, Belgium

Received: 19 February 2009 – Accepted: 23 March 2009 – Published: 8 April 2009

Correspondence to: H. Herbin (herve.herbin@univ-lille1.fr)

Published by Copernicus Publications on behalf of the European Geosciences Union.

Abstract

In this paper we analyze distributions of water vapour isotopologues in the troposphere using infrared spectra recorded by the Infrared Atmospheric Sounding Interferometer (IASI), which operates onboard the Metop satellite in nadir geometry. The simultaneous uncorrelated retrieval of $H_2{}^{16}O$ and HDO was performed on radiance measurements using a line-by-line radiative transfer model and an inversion procedure based on the Optimal Estimation Method (OEM). The characterizations of the retrieved products in terms of vertical sensitivity and error budgets show that IASI measurements contain up to 6 independent pieces of information on the vertical distribution of $H_2{}^{16}O$ and up to 3.5 for HDO from the surface up to the upper troposphere (0–20 km). The $H_2{}^{16}O$ retrieved profiles are in good agreement with local sonde measurements at different latitudes during different times of the year. Our results demonstrate the ability of the IASI instrument to monitor atmospheric isotopologic water vapour distributions with unprecedented sensitivity. As a case study, we analyse concentration distributions and spatio-temporal variations of $H_2{}^{16}O$ and HDO during the October 2007 Krosa super-typhoon over South-East Asia and show with this example the IASI potential to capture variations in the HDO/$H_2{}^{16}O$ isotopologic ratio values over space and time.

1 Introduction

Water vapour is the most important atmospheric trace gas and a key compound of the global climate (Ciais et al., 2004; Gedzelman et al., 2003; Hartmann, 2002; Lawrence et al., 2002; Smith, 1992). It plays an important role in many atmospheric processes, such as radiative transfer, circulation dynamics (Strong et al., 2007; Hanisco et al., 2007; Kuang et al., 2003; Johnson et al., 2001; Moyer et al., 1996), stratospheric chemistry (Steinwagner et al., 2007; Rosenlof et al., 2001, 2003; McCarthy et al., 2004; Franz et al., 2005; Coffey et al., 2006), cloud formation (Schmidt et al., 2005; Webster et al., 2003), precipitation (Bowen and Revenaugh, 2003) and the green-

ACPD

9, 9267–9290, 2009

house effect (Schneider et al., 1999; Hartmann, 2002). There are several stable isotopologic species of the water molecule ($H_2{}^{16}O$, $H_2{}^{18}O$, $H_2{}^{17}O$ and HDO being the most abundant), each with different vapour pressures and reaction rates. The isotopic composition is given in per mil (‰) units using the conventional δ notation relative to the V-SMOW standard, where

$$\delta = \left(\frac{R}{R_{\mathrm{SMOW}}} - 1 \right) \times 1000 ,$$

and R denotes the isotopologic mass ratio, with R_{SMOW}=[HDO]/[$H_2{}^{16}O$]= 0.31152×10^{-3}. The isotopologic water vapour composition is strongly affected by evaporation sources and condensation conditions. Isotopologic measurements are therefore important for the analysis of hydrologic processes and for studies on the history of air masses (Bechtel and Zahn, 2003). Although an accurate knowledge of the different water isotopologues distributions is needed for studying dehydration mechanisms, there are few measured tropospheric profiles of the heavier isotopologues of water vapour (Zahn et al., 2006, and references therein). Especially satellite observations, which would offer distributions over large regions, are missing. This is mainly due to the large variability of water vapour concentrations both in space and time.

In a previous paper, we have demonstrated the ability of space-borne infrared sounders to measure simultaneously the vertical profiles of the main water isotopologues (i.e. $H_2{}^{16}O$, $H_2{}^{18}O$ and HDO) and their ratios (Herbin et al., 2007). These results were obtained using the infrared spectra recorded by the Interferometric Monitor for Greenhouse gases (IMG) instrument. Likewise, distributions of the tropospheric HDO/$H_2{}^{16}O$ ratio were reported using measurements from the Tropospheric Emission Spectrometer (TES) (Worden et al., 2006 and 2007) and these have been used to study the hydrologic processes over continental regions (Brown et al., 2008). Improved sounding performances are expected for measurements from the recently launched IASI sounder, which, as an operational meteorological instrument onboard the European MetOp-A platform, targets primarily temperature and water vapour profile mea-

surements in the troposphere (Clerbaux et al., 2008; Schlüssel et al., 2005).

Here, we present the first simultaneous retrievals of $H_2{}^{16}O$ and HDO vertical distributions from IASI. The goal of this preliminary study is to characterize the capabilities of the IASI in providing information on concentration distributions of $H_2{}^{16}O$, HDO but also on the more challenging δ_D.

In the next section, we describe briefly the IASI instrument, the measured radiance spectra and the retrieval method. Section 3 presents tropospheric (0–20 km) vertical distributions for a selection of IASI spectra coincident with data from radiosondes (Gaffen, 1994) and representative for different latitudes and seasons. The retrieved profiles are discussed with respect to the error budgets and the vertical sensitivity of the measurements. We also examine in this section the advantage of using, for the HDO retrievals, the reflected solar part of the spectrum for the inversion process. In Sect. 4 we use the unprecedented spatial and temporal sampling of IASI to probe the regional isotopic composition of water during a major meteorological event (Krosa Typhoon in early October 2007) and discuss the capabilities of the instrument to capture useful δ_D variations, notably in the perspective to improve on the monitoring our environment. Section 5 summarizes our results and presents perspectives on future applications.

2 Measurements and methods

2.1 Measurements

IASI is one of the eleven instruments launched onboard the polar sun-synchronous orbiting Metop-A platform on 19 October 2006. The IASI instrument (Clerbaux et al., 2007, 2009; Schlüssel et al., 2005) is a nadir-viewing Fourier transform interferometer which records the thermal infrared emission of the Earth-atmosphere system between 645 and 2760 cm^{-1} with an apodized spectral resolution of 0.5 cm^{-1}. IASI's field of view corresponds to a 2×2 pixel matrix where at nadir each pixel has a 12 km footprint

ACPD
9, 9267–9290, 2009

on the ground. Its ability to scan across a swath of 2200 km allows for global coverage twice a day with a good horizontal resolution. The IASI specifications are ideal for studying the atmosphere from a local to a global scale. The main purpose of the IASI mission is to provide temperature and tropospheric water vapour profiles with of 1 K, 10–15% accuracies and with 1 and 2 km vertical resolutions, respectively (Clerbaux et al., 2007, 2009; Schlüssel et al., 2005).

2.2 Data analysis

The $H_2{}^{16}O$ and HDO profiles are retrieved from the IASI spectra using the *Atmosphit* software developed at the Université Libre de Bruxelles. This software is based on a detailed line-by-line radiative transfer model, including ray tracing for various geometries and a retrieval scheme relying on the Optimal Estimation Method (OEM) (Rodgers, 2000). The theoretical elements relevant for the present study are similar to those described by (Barret et al., 2005; Coheur et al., 2005; Herbin et al., 2007). For the retrievals, the water vapour a priori covariance matrices $\boldsymbol{S}_a$ and the a priori state vector $\boldsymbol{x}_a$ are built based on local radiosondes data over 2 months (day and night) and averaged on 5 different latitudinal bands (+90°, +60°), (+60°, +23°), (+23°, −23°), (−23°, −60°) and (−60°, −90°). The a priori information covers altitudes ranging from the ground up to 20 km, interpolated on a grid of 2 km. The spectroscopic parameters were extracted from the HITRAN 2004 database (Rothman et al., 2005). Because the signal to noise ratio varies over the IASI spectra (see Fig. 1), we use for the retrievals a diagonal $\boldsymbol{S}_\varepsilon$ matrix ($\boldsymbol{S}_\varepsilon=\sigma_\varepsilon \boldsymbol{I}$), with a value of σ_ε close to the best Root Mean Squares (RMS) of typical retrievals, i.e. $\sigma_\varepsilon=2\times10^{-6}\,\mathrm{W/cm^2\,sr\,cm^{-1}}$.

Water vapour isotopologues absorb almost everywhere in the spectral range of IASI, with many strong lines that saturate the absorption signal throughout the ν_2 band. For this reason, we have selected two spectral windows for the simultaneous retrieval of $H_2{}^{16}O$ and HDO, extending, respectively from 1186.95 to 1300.75 and 1307.25 to 1406.40 $\mathrm{cm^{-1}}$, located both on the long wavelength end of the ν_2 band. IASI spectra

cover also parts of the infrared above 2500 cm^{-1}, where the upwelling source function during daytime is dominated by the reflected solar radiation. Absorption of this radiation is mainly attributable to methane (CH_4) and HDO. It therefore offers a potential improvement on the sensitivity of IASI to these species in the lowest layers of the atmosphere (see e.g. Razavi et al., this issue). To analyze this for HDO, we have used a supplemental spectral window extending from 2588.00 to 2757.30 cm^{-1}. For sake of illustration, Fig. 1 gives an example of a spectral fit in the selected windows, showing also the typical quality of the residual spectra (Observed-Calculated).

The retrievals use along with water vapour, the Level 2 pressure and temperature profiles from the operational processing at Eumetsat. In the inversion step, the volume mixing ratios (vmr) for water isotopologues are retrieved on 10 discrete vertical layers, extending from the ground up to 20 km as 0–1, 1–3, 3–5, 5–7, 7–9, 9–11, 11–13, 13–15, 15–17 and 17–20 km. In the spectral range used, the surface temperature, the proportion of reflected solar radiation ("reflectivity"), the total columns of $H_2{}^{17}O$, CO_2, N_2O, CH_4 and HNO_3, and the profiles of $H_2{}^{16}O$, HDO and $H_2{}^{18}O$ are adjusted simultaneously. Although interesting information on $H_2{}^{18}O$ is obtained as well with 3–4 degrees of freedom for signal (DOFS), the calculation of the delta parameter is more challenging, because of the smaller ranges of values. They will therefore not be discussed here.

3 Retrievals and characterization

The goal of this section is to characterize the capabilities of IASI to obtain vertically resolved profiles of $H_2{}^{16}O$, HDO and δ_D from the ground up to the upper troposphere/lower stratosphere region.

In order to quantify the benefit of the shortwave retrieval window above 2500 cm^{-1} for the HDO profile, we have performed a series of retrievals on IASI spectra significantly affected by the reflection of the solar radiation. Figure 2 shows an example of

ACPD
9, 9267–9290, 2009

HDO error budgets and averaging kernels resulting from the inversion of a IASI observation at Southern mid-latitude above the ocean, in December 2007, performed with (upper panel) and without (lower panel) the supplemental shortwave window. The degrees of freedom for the signal, which give an estimate of the independent pieces of information contained in the measurements (Rodgers, 2000) are, respectively 3.01 and 2.61. These highlight mainly the gain of information on HDO close to the surface from using the reflected solar radiation, with the error at ground-level decreasing from 19% to 13% for the case shown in Fig. 2. Interestingly, the retrieved $H_2{}^{16}O$ profile is also slightly improved following this procedure. Despite only a small number of IASI spectra show sufficient signal-to-noise above 2500 cm^{-1} to benefit the HDO retrieval, taking into account this additional spectral window was shown not to degrade the retrieval performances in other cases. It was therefore kept in all further analyses.

To assess the quality of the water vapour retrievals, we have first chosen to compare the retrieved profiles to a set of humidity soundings at 6 sites, representative of different latitudes (Table 1) on a same day (1 September 2008). The water vapour radiosonde data have been provided by the Wyoming University. The co-localisation criteria were set on the spatial scale to 1° latitude and 1° longitude from the six stations and on the temporal scale to within twelve hours of the soundings (Tables 1 and 2).

Figure 3 shows the profile comparison between the $H_2{}^{16}O$ retrievals, the humidity soundings, the IASI Level 2 delivered operationally at for each scene and the a priori profiles (left panel). It shows in addition the averaging kernels and the error budgets for each isotopologue at each site, as well as the calculated δ_D value (right panel) of the coincident IASI/sonde water vapour measurement of Table 1. In all cases, we find that the $H_2{}^{16}O$ retrieved profiles are in good agreement with the sonde values (averaged deviation at ground level: 17.5%) over the entire altitude range (averaged deviation between 0 and 20 km: 7.2%) and in particular that they reproduce well the large vertical gradient. We also conclude, recalling that all observations are made on the same day, that the retrieved profiles adequately capture the large latitudinal variability. For tropical scenes (at Darwin and Kingston), the volume mixing ratio are

ACPD
9, 9267–9290, 2009

for instance almost one order of magnitude larger than for the regions with the highest latitude (at Novolazarevskaja and Bjornoya).

The HDO profiles from the same scene have been retrieved from a priori profiles constructed from the $H_2{}^{16}O$ ones, divided by the SMOW ratio and corrected by the Rayleigh distillation model (Zhang et al., 2005). The HDO retrieved profiles have a similar vertical structure as the corresponding $H_2{}^{16}O$ profiles (Fig. 3), despite weaker vertical sensitivity. In fact, the averaging kernels or $H_2{}^{16}O$ reveal a maximum sensitivity in the tropics and also at mid-latitudes during daytime, with an integrated kernel function spanning the entire altitude range from the surface to 14 km, degrading to 2–12 km at mid-latitudes during night-time. For the highest latitudes there is sensitivity only between 2 and 10 km. Similarly for HDO, the measurements are sensitive between the ground level and 12 km for tropical and mid-latitude regions during the day but from 2 and 12 km during the night. At the higher latitudes the sensitivity to HDO is mostly between 2 and 8 km. This dependency of the measurements to the water vapour vertical structure is confirmed by the degrees of freedom, listed in the Table 1. One result that already follows is that the information on the isotopologic ratio, which will be discussed next, is obviously limited by HDO, which has the lowest information content. For each case of Fig. 3, the error profile budget is also displayed. The different curves correspond to the square root of the diagonal elements of the measurement error, the smoothing error and the model parameter error covariance matrices (Herbin et al., 2007). The error analysis confirms that the retrievals are mainly driven by a priori information above 16 km for both isotopologic species. For $H_2{}^{16}O$, the total error is mostly below 15% over the entire altitude range of the troposphere, increasing to 26% near the surface in the situations where the measurements are less sensitive (highest latitudes). This total error is evenly distributed between the smoothing and the measurements errors, with additional contributions from uncertainties on model parameters being essentially negligible. It is interesting to note the accuracy that we obtain for $H_2{}^{16}O$ tropospheric profiles is quite good in comparison to the expected one (Clerbaux et al., 2007, 2009; Schlüssel et al., 2005). For HDO the error on the profile vary

between 25 and 40%, with the smoothing error becoming very dominant. As could be anticipated from the discussion above, the total error is particularly small when the sensitivity is high, with errors reaching, for instance, 3% for $H_2{}^{16}O$ and 9% for HDO at the ground level at Kingston. In all cases and for both isotopologues, the retrieval makes a substantial improvement with respect to the a priori variability. The most significant improvement is in the troposphere between 4 and 8 km, where the a priori uncertainty is largest. To end this sensitivity overview, it is interesting to note here the difference in sensitivity between the two tropical locations (Darwin and Kingston) recorded, respectively during the day and the night, which is illustrative for the improvement due to the shortwave retrieval window. It is also worth stressing out that the present analysis shows similarities with the results previously obtained from IMG (Herbin et al., 2007). With IASI we do find, however, a higher vertical sensitivity for both isotopologues, likely due to the better signal to noise ratio of the spectra.

The profiles of the two isotopologues displayed in Fig. 3 do not allow, as such, the detection of any unexpected evolution in the isotopologic vertical distribution. For this purpose, the calculation of the δ_D values is a prerequisite (Fig. 3, right panel). In the light of the averaging kernels and error budgets, we have restricted the study of the isotopologic depletion to altitudes ranging between 0 and 10 km. The resulting vertical distributions exhibit the expected general decay of δ_D with altitude. Interestingly the retrieved values and their uncertainties are consistent with those reported in the literature, with different experimental techniques (Gettelman et al., 2005; Ehhalt et al., 2005), thus showing the capabilities of IASI to follow the isotopologic variations in water vapour from local to global scales on a daily basis.

Also temporal variations in δ_D can be captured, as illustrated in Fig. 4, which shows profiles, error budgets and averaging kernels above Hawaii as an illustration of the seasonal variations in tropical regions. The $H_2{}^{16}O$ and HDO profiles do not show seasonal variations, as expected for tropical latitude but the calculated δ_D profiles show a large variability around the a priori profiles, with for example δ_D ground level values positive in June and September and negative for the coldest months (December and

March).

4 Case study

In the previous section we have demonstrated that IASI spectra contain significant information on the distributions of $H_2{}^{16}O$, HDO and their ratio, with exceptional spatial resolution and a revisit time two times per day. This opens perspective for studying atmospheric dynamical and climatic processes, which were not accessible from space observations before. In order to illustrate this, we have chosen to perform a detailed study of the δ_D partitioning on a regional scale, during a typhoon, which is accompanied by extreme and complex hydrologic processes. The Krosa Typhoon, which was one of the major meteorological events of the year 2007, is taken as a case study. The sequence was as follows:

It initially formed on 1 October as a tropical depression southeast of the Philippines. Rapid intensification took place and the depression was upgraded to a tropical storm and later a typhoon. As it intensified, it gained a wide eye and moved northwest, becoming a super typhoon on 5 October when it approached Taiwan. It slowly weakened afterwards before making landfall in Taiwan and southeast China. The sequence is considered to have ended three days later, on 8 October, above the Philippine Sea.

For the retrievals of the isopologues during the 8 days of this event, we have selected cloud free spectra. Only scenes showing a degree of homogeneity larger than 90% have been kept, thus removing all cloudy spectra just above and around the Typhoon's eye. The resulting distributions, presented in Fig. 5 are averages on a 1° latitude by 1° longitude grid. The full black circles in Fig. 5 show the location of the typhoon eye and the white zones identify the cloudy areas. We focus hereafter on the tropospheric distributions $H_2{}^{16}O$ and δ_D, expressed as an integrated column from 0 to 8 km such as to use the vertical range where each species is more sensitive. The retrieved $H_2{}^{16}O$ map for 3 October, reveals two moist fronts: one in the Southeast linked to typhoon approach, and one above the Philippines corresponding to the end of the tropical storm

ACPD
9, 9267–9290, 2009

Lekima which occurred in that region 27 September to 5 October. On 8 October the map shows again two moist fronts but now in the Northwest, the one closest to the typhoon eye being more important. The δ_D map for 3 October is quite standard and does not reveal particular features when compared to the $H_2{}^{16}O$ distribution. On the contrary, the δ_D map on 8 October is quasi opposite to that of $H_2{}^{16}O$. For the regions where δ_D values are very low the humidity tends to be very high, likely pointing to an intense depletion in the deuterated isotopologue after the typhoon passed.

To further highlight this, Fig. 6 shows δ_D values as a function of the relative humidity for 8 October. Full and empty circles represent the morning and afternoon data, respectively. Rayleigh distillation lines originating from air parcels with saturation specific humidity values based on oceanic temperatures of 288 and 300 K, and initial δ_D values of −79‰ (vapour equilibrium with the ocean) are shown as black lines. The grey lines represent the enriching effects that arise from mixing moist marine with drier air parcels. These curves are based on typical tropical surface temperature of 288 K (for more details, see supplemental material of Worden et al., 2007).

The large variability of the δ_D values suggests important mixing processes, including turbulent transport and large scale advection over the analyzed region. Although 51% of the measurements are constrained by Rayleigh distillation lines and 18% by evaporation lines, many points (31%) are more depleted than predicted by Rayleigh distillation model. This suggests that observations result from an accumulation of condensation processes, with large isotopic exchange occurring during heavy rainfall.

5 Conclusions

A set of high–resolution Fourier transform nadir spectra measured by the IASI instrument have been analyzed to obtain vertical tropospheric distributions of two isotopologic species of water vapour ($H_2{}^{16}O$ and HDO) and their ratio. The retrievals were made using software relying on the OEM, allowing to measure volume mixing ratios and partial columns from the ground up to 20 km. The analysis shows the sensitivity

ACPD
9, 9267–9290, 2009

of IASI to be highest between the surface and 8 km. At these altitudes, the uncertainties are less than 20% on each retrieved level of the profile for the principal isotopologue and 30% for HDO for low and mid-latitudes, independently of the season. The uncertainties are larger at high latitudes because of the lower humidity and spectral radiances.

The comparison of the retrieved profiles with coincident sonde measurements, performed at a series of representative latitudes and seasons, has revealed the potential of IASI to capture the spatial variations of water vapour in the troposphere. The characterization of the profiles showed that the measurements contain up to 6 ($H_2{}^{16}O$) and 3.5 (HDO) independent pieces of information on the vertical distributions. The advantage of using the solar reflected part of spectra to improve the low layer information of HDO during daytime is also shown.

The $H_2{}^{16}O$ and δ_D zonal distributions of partial columns above Southeast Asia during a major meteorological event (Krosa super typhoon) have been studied. Significant horizontal variations of the δD values during the Typhoon sequence are found, and in particular a very high depletion of the δ_D values after the typhoon crossing has been observed. The analysis of δ_D as a function of H_2O for that event has revealed that about one third of the measurements are not following the Rayleigh model, thus allowing for a distinction between evaporation and condensation processes.

Globally, the results have demonstrated the ability of the IASI instrument to measure $H_2{}^{16}O$ and HDO profiles accurately and with a good coverage and sampling. These results open promising perspectives for analyses of meteorological processes on extended spatial scales and over longer periods.

Acknowledgement. IASI has been developed and built under the responsibility of the Centre National d'Etudes Spatiales (CNES, France). It is flown onboard the Metop satellites as part of the EUMETSAT Polar System. The IASI L1 data are received through the EUMETCast near real time data distribution service. The research in Belgium was funded by the F.R.S.-FNRS (M.I.S. nF.4511.08), the Belgian State Federal Office for Scientific, Technical and Cultural Affairs and the European Space Agency (ESA-Prodex arrangements C90-327). Financial support by

the “Communauté française de Belgique – Actions de Recherche Concertées” is also acknowledged. C. Clerbaux acknowledge CNES for the financial support.

References

Barret, B., Turquety, S., Hurtmans, D., Clerbaux, C., Hadji-Lazaro, J., Bey, I., Auvray, M., and Coheur, P.-F.: Global carbon monoxide vertical distributions from spaceborne high-resolution FTIR nadir measurements, Atmos. Chem. Phys., 5, 2901–2914, 2005, http://www.atmos-chem-phys.net/5/2901/2005/.

Bechtel, C. and Zahn, A.: The isotopologue composition of water vapour: A powerful tool to study transport and chemistry of middle atmospheric water vapour, Atmos. Chem. Phys. Discuss., 3, 3991–4036, 2003, http://www.atmos-chem-phys-discuss.net/3/3991/2003/.

Bowen, G. J. and Revenaugh, J.: Interpolating the isotopologic composition of modern meteoric precipitation, Water Resour. Res., 39(10), 1299, doi:10.1029/2003WR002086, 2003.

Brown, D., Worden, J., and Noone, D.: Comparison of hydrology over convective continental regions using water vapor isotope measurements from space, J. Geophys. Res., 113, D15124, doi:10.1029/2007JD009676, 2008.

Ciais, P. and Jouzel, J.: Deuterium and oxygen 18 in precipitation: Isotopologic model, including mixed cloud processes, J. Geophys. Res., 99(D8), 16793, doi:10.1029/94JD00412, 1994.

Clerbaux, C., Hadji-Lazaro, J., Turquety, S., George, M., Coheur, P.-F., Hurtmans, D., Wespes, C., Herbin, H., Blumstein, D., Tournier, B., and Phulpin, T.: The IASI/MetOp mission: first observations and highlight of its potential contribution to the GMES Earth observation component, Space Res. Today, 168, 19–24, 2007.

Clerbaux, C., Boynard, A., Clarisse, L., George, M., Hadji-Lazaro, J., Herbin, H., Hurtmans, D., Pommier, M., Razavi, A., Turquety, S., Wespes, C., and Coheur, P.-F.: Monitoring of atmospheric composition using the thermal infrared IASI/MetOp sounder, Atmos. Chem. Phys. Discuss., 9, 8307–8339, 2009, http://www.atmos-chem-phys-discuss.net/9/8307/2009/.

Coffey, M. T., Hannigan, J. W., and Goldman, A.: Observations of upper tropospheric/ lower stratospheric water vapour and its isotopologues, J. Geophys. Res., 111(D14), D14313, doi:10.1029/2005JD006093, 2006.

Coheur, P.-F., Barret, B., Turquety, S., Hurtmans, D., Hadji-Lazaro, J., and Clerbaux, C.: Retrieval and characterization of ozone vertical profiles from a thermal infrared nadir sounder, J. Geophys. Res., 110(D24), D24303, doi:2005JD005845, 2005.

Ehhalt, D. H., Rohrer, F., and Fried, A.: Vertical profiles of HDO/H_2O in the troposphere, J. Geophys. Res., 110(D13), D13301, doi:2004JD005569, 2005.

Franz, P. and Rckmann, T.: High-precision isotope measurements of $H_2{}^{16}O$, $H_2{}^{17}O$, $H_2{}^{18}O$, and the δ^{17}O-anomaly of water vapor in the southern lowermost stratosphere, Atmos. Chem. Phys., 5, 2949–2959, 2005, http://www.atmos-chem-phys.net/5/2949/2005/.

Gaffen, D.: Temporal inhomogeneities in radiosonde temperature records, J. Geophys. Res., 99(D2), 3667–3676, 1994.

Gedzelman, S., Hindman, E., Zhang, X., Lawrence, J., Gamache, J., Black, M., Black, R., Dunion, J., and Willoughby, H.: Probing Hurricanes with stable isotopologues of rain and water vapour, Mon. Weather Rev., 131, 1112–1127, 2003.

Gettelman, A. and Webster, C. R.: Simulations of water isotopologue abundances in the upper troposphere and lower stratosphere and implications for stratosphere troposphere exchange, J. Geophys. Res., 110(D17), D17301, doi:10.10.29/2004JD004812, 2005.

Hanisco, T. F., Moyer, E. J., Weinstock, E. M., St. Clair, J. M., Sayres, D. S., Smith, J. B., Lockwood, R., and Anderson, J. G.: Observations of deep convective influence on stratospheric water vapor and its isotopic composition, Geophys. Res. Let., 34, L048141–L048145, 2007.

Hartmann, D. L.: Climate change: tropical surprises, Science, 295, 811–812, 2002.

Herbin, H., Hurtmans, D., Turquety, S., Wespes, C., Barret, B., Hadji-Lazaro, J., Clerbaux, C., and Coheur, P.-F.: Global distributions of water vapour isotopologues retrieved from IMG/ADEOS data, Atmos. Chem. Phys., 7, 3957–3968, 2007, http://www.atmos-chem-phys.net/7/3957/2007/.

Johnson, D. J., Jucks, K. W., Traub, W. A., and Chance, K. V.: Isotopic composition of stratospheric water vapor: Implications for transport, J. Geophys. Res., 106(D11), 12219–12226, 2001.

Kuang, Z. M., Toon, G. C., Wennberg, P. O., and Yung, Y. L.: Measured HDO/H_2O ratios across the tropical tropopause, Geophys. Res. Lett., 30(7), 1372, doi:10.1029/2003GL017023, 2003.

Lawrence, J. R., Gedzelman, S. D., Gamache, J., and Black, M.: Stable isotopologue ratios: Hurricane Olivia, J. Atmos. Chem., 41, 67–82, 2002.

McCarthy, M. C., Boering, K. A., Rahn, T., Eiler, J. M., Rice, A. L., Tyler, S. C., Schauffler, S., Atlas, E., and Johnson, D. G.: The hydrogen isotopologic composition of water vapour entering the stratosphere inferred from high-precision measurements of δ_D-CH_4 and δ_D-H_2, J. Geophys. Res., 109(D07), D07304, doi:10.10.29/2003JD004003, 2004.

Moyer, E. J., Irion, R. W., Yung, Y. L., and Gunson, M. R.: ATMOS stratospheric deuterated water vapour and implications for troposphere-stratosphere transport, Geophys. Res. Lett., 23(17), 2385, doi:10.10.29/1996GL01489, 1996.

Razavi, A., Clerbaux, C., Wespes, C., Clarisse, L., Hurtmans, D., Payan, S., Camy-Peyret, C., and Coheur, P. F.: Characterization of methane retrievals from the IASI space-borne sounder, Atmos. Chem. Phys. Discuss., 9, 7615–7643, 2009, http://www.atmos-chem-phys-discuss.net/9/7615/2009/.

Rodgers, C. D.: Inverse Methods for Atmospheric Sounding: Theory and Practice, World Scientific, Hackensack, NJ, 2000.

Rosenlof, K. H., Oltmans, S. J., Kley, D., Russell, J. M., Chiou, E.-W., Chu, W. P., Johnson, D. G., Kelly, K. K., Michelsen, H. A., Nedoluha, G. E., Remsberg, E. E., Toon, G. C., McCormick, M. P.: Stratospheric water vapour increases over the past half-century, Geophys. Res. Lett., 28(7), 1195, doi:10.10.29/2000GL012502, 2001.

Rosenlof, K. H.: How water enters the stratosphere, Science, 302, 1691–1692, 2003.

Rothman, L. S. et al.: The HITRAN 2004 molecular spectroscopic database, J. Quantitative Spectrosc. Radiat. Transf., 96, 139–204, 2005.

Schlüssel, P., Hultberg, T. H., Phillips, P. L., August, T., and Calbet, X.: The operational IASI Level 2 processor, Adv. Space Res., 36, 982–988, 2005.

Schmidt, G. A., Hoffmann, G., Shindell, D. T., and Hu, Y.: Modelling atmospheric stable water isotopologues and the potential for constraining cloud processes and stratosphere-troposphere water exchange, J. Geophys. Res., 110(D21), D21314, doi:10.1029/2005JD005790, 2005.

Schneider, E. K., Kirtman, B. P., and Lindzen, R. S.: Tropospheric Water Vapour and Climate Sensitivity, J. Atmos. Sc., 56, 1649–1658, 1999.

Smith, R. B.: Deuterium in North Atlantic storm tops, J. Atmos. Sc., 49, 2041–2057, 1992.

Steinwagner, J., Milz, M., von Clarmann, T., Glatthor, N., Grabowski, U., Höpfner, M., Stiller, G. P., and Röckmann, T.: HDO measurements with MIPAS, Atmos. Chem. Phys., 7, 2601–2615, 2007, http://www.atmos-chem-phys.net/7/2601/2007/.

Strong, M., Scharp, Z. D., and Gutzler, D. S.: Diagnosing moisture transport using D/H ratios of water vapor, Geophys. Res. Lett., 34, L03404, doi:10.1029/2006GL028307, 2007.

University of Wyoming' department of atmospheric sciences radiosondes data base http://weather.uwyo.edu/upperair/sounding.html

Webster, C. R. and Heymsfield, A. J.: Water isotopologue ratios D/H, $^{18}O/^{16}O$, $^{17}O/^{16}O$ in and out of clouds map dehydration pathways, Science, 302, 1742–1745, 2003.

Worden, J., Bowman, K., Noone, D., et al.: Tropospheric Emission Spectrometer observations of the tropospheric HDO/H2O ratio: Estimation approach and characterization, J. Geophys. Res., 111(D16), D16309, doi:2005JD006606, 2006.

Worden, J., Noone, D., Bowman, K., et al.: Importance of rain evaporation and terrestrial sources in the tropical water cycle, Nature, 445, 528-553, 2007.

Zahn, A., Franz, P., Bechtel, C., Grooß, J.-U., and Röckmann, T.: Modelling the budget of middle atmospheric water vapour isotopologues, Atmos. Chem. Phys., 6, 2073–2090, 2006, http://www.atmos-chem-phys.net/6/2073/2006/.

Zhang, X., Tian, L., and Liu, J.: Fractionation mechanism of stable isotope in evaporating water body, J. Geophys. Sci., 15, 375–384, 2005.

Table 1. Coincident IASI and water vapour sonde measurements for six locations (identified by name, latitude, longitude) on the 1 September 2008. The DOFS for $H_2{}^{16}O$ and HDO are given at each site. Numbers in parentheses for sun reflectance parameter are the standard deviation in units of the least significant digits.

Observing site	Latitude, longitude	Day/night	Sun "reflectivity"	$H_2{}^{16}O$ DOFS	HDO DOFS
Novolazarevskaja	–70.76, 11.82	Day	5×10^{-8} (4)	3.80	1.34
Santo Domingo	–33.61, –71.62	Day	1.5×10^{-7} (0.3)	5.18	2.88
Darwin	–12.42, 130.88	Night	0	5.86	3.37
Kingston	18.06, –76.84	Day	1.2×10^{-7} (0.3)	5.91	3.50
Hailar	49.22, 119.75	Day	3.0×10^{-7} (0.3)	5.09	3.03
Bjornoya	74.51, 19.02	Night	0	4.05	2.15

ACPD
9, 9267–9290, 2009

Table 2. DOFS of coincident IASI and water vapour sonde measurements above Hawaii (+19.72°, −155.05°) for selected days in Septeber 2008, December 2007, March and June 2008.

Dates	$H_2{}^{16}O$ DOFS	HDO DOFS
21 Sep 2008	5.73	3.09
21 Dec 2007	5.91	3.35
28 Mar 2008	5.81	3.26
21 Jun 2008	5.65	3.07

ACPD
9, 9267–9290, 2009

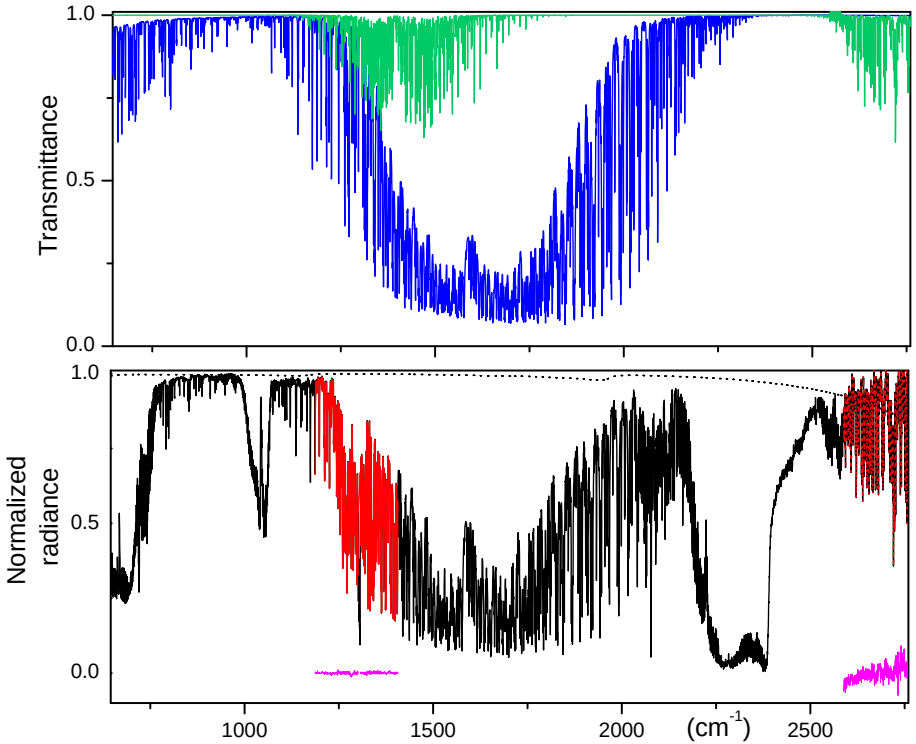

Fig. 1. Retrieval spectral windows. *Top*: $H_2{}^{16}O$ (Blue) and HDO (Green) transmittance spectra. *Bottom*: IASI measured spectrum (normalized radiance, in black) and fitted spectrum (red) in the spectral windows used for retrieving $H_2{}^{16}O$ and HDO profiles. The magenta lines show the residual (observed-calculated) spectra. The average IASI noise is indicated by a black dashed line.

ACPD
9, 9267–9290, 2009

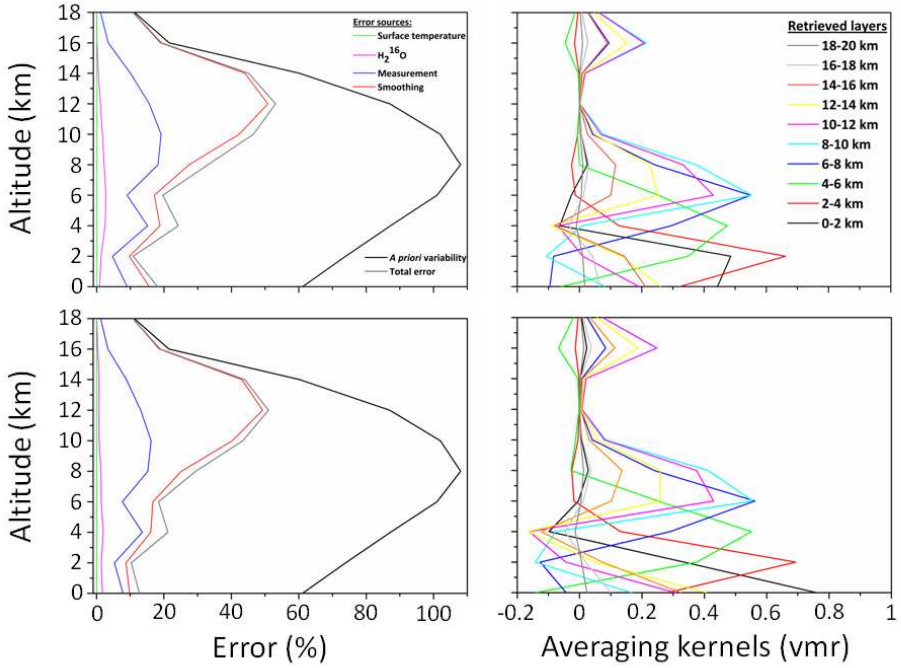

Fig. 2. HDO profile retrieval characterization for a mid-latitude scene with (*bottom*) and without (*top*) taking into account the shortwave window in the retrieval procedure.
Left: Error profiles. The curves are the square root of the diagonal elements of the *prior* and *posterior* error covariance matrices. The errors due to uncertainties on the temperature profiles are calculated assuming an uncorrelated uncertainty of 1 K. The errors associated with the uncertainties on the others species (i.e. $H_2{}^{17}O$, $H_2{}^{18}O$, CH_4, CO_2, N_2O, HNO_3) are negligible and therefore not shown. *Right*: Averaging kernels, in volume mixing ratio units for the ten retrieved layers. Degrees of freedom for signal are, respectively 3.01 and 2.61 with or without the shortwave band taken into account.

ACPD
9, 9267–9290, 2009

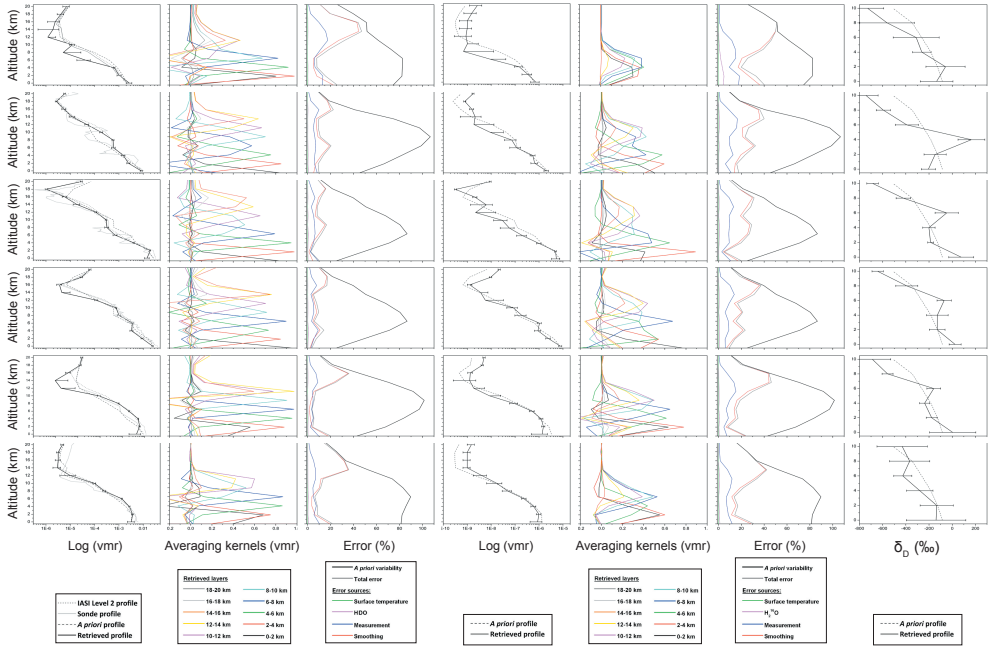

Fig. 3. *Left*: Retrieved $H_2{}^{16}O$ profiles (vmr) up to 20 km from IASI observations made on the 1 September 2008 for six different sites (see Table 1); averaging kernels, in volume mixing ratio units, for each retrieved layers and error profiles. *Middle*: The same three graphics for HDO. *Right*: δ_D profiles in ‰ unit between 0 and 10 km. For profiles, the grey and black lines represent the sonde and retrieved profiles, respectively. The black dashed and dot lines are the a priori and the Level 2 IASI profiles, respectively. The a priori profiles for HDO have been constructed from those of $H_2{}^{16}O$ relying on the Rayleigh distillation model (see text for details). The corresponding degrees of freedom for signal are reported in Table 1.

ACPD
9, 9267–9290, 2009

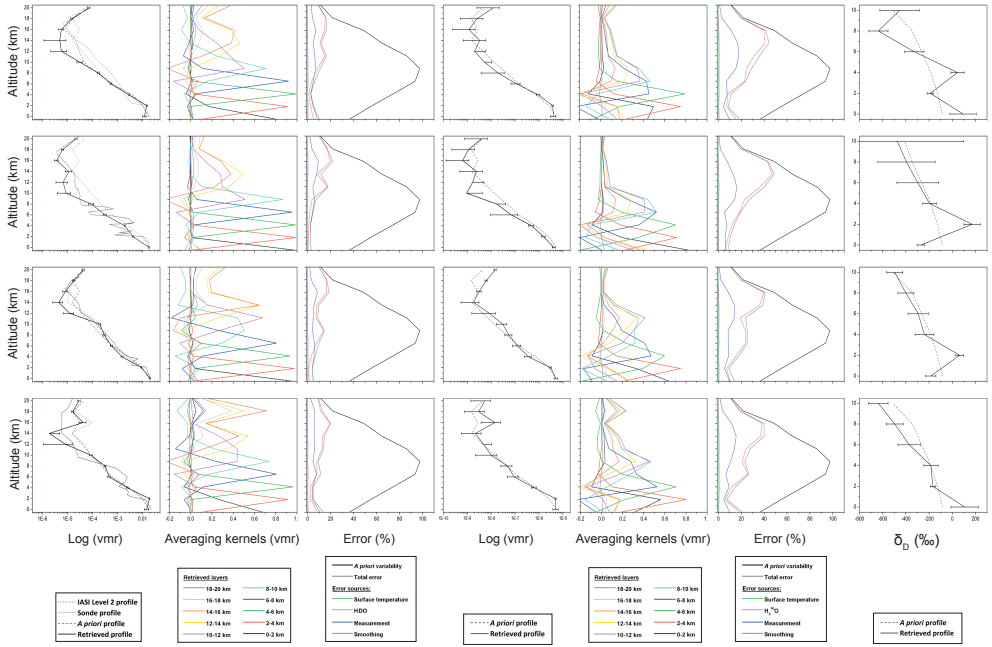

Fig. 4. Same as Fig. 3 for $H_2{}^{16}O$ and HDO profiles (vmr) retrieved from IASI observations at Hawaii on four days (*top to bottom*): 21 September 2008, 21 December 2007, 28 March 2008 and 21 June 2008. The corresponding DOFS are reported in Table 2.

ACPD
9, 9267–9290, 2009

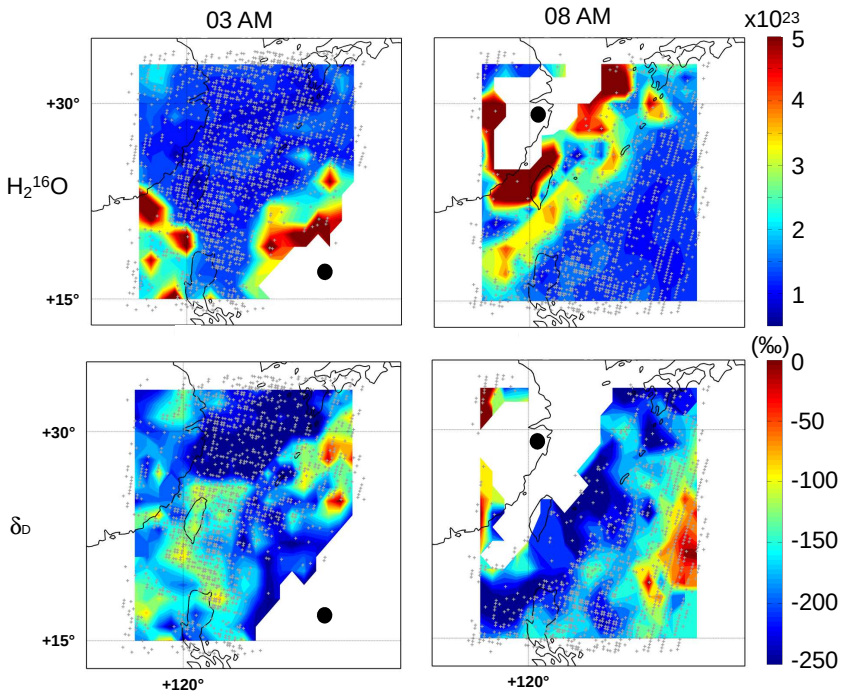

Fig. 5. Distribution of $H_2{}^{16}O$ and δ_D for the mornings of the 3 and 8 October 2007. $H_2{}^{16}O$ distributions are given as partial columns (0–8 km) in 10^{23} molec cm^{-2}. δ_D distributions are in ‰ unit averaged on the (0–8 km) partial column. Data are averaged on a 1°×1° longitude-latitude grid. The grey crosses show the location of the IASI retrievals. The full black circles show the location of the typhoon eye and the white zones identify the cloudy areas.

ACPD
9, 9267–9290, 2009

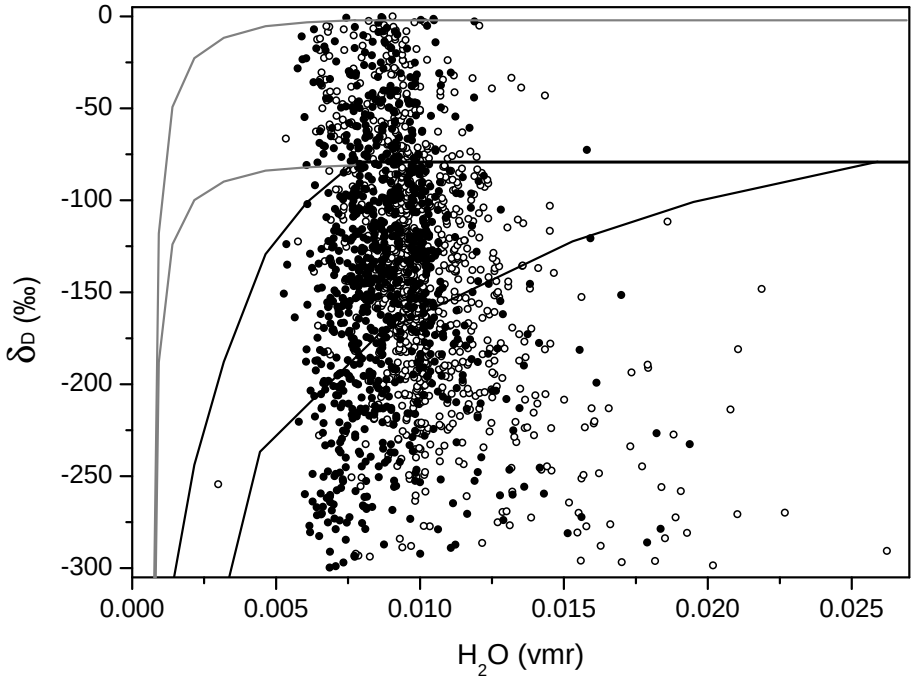

Fig. 6. δ_D (‰) as a function of $H_2{}^{16}O$ (vmr) for the 8 October 2007 during Krosa typhoon overpass in South-East Asia. The empty and full black circles show, respectively the morning and evening data. The black lines represent the Rayleigh distillation curves with surface temperatures of 288 K (left line) and 300 K (right line), initialized to the surface layer δ_D value of −79‰. The grey lines represent evaporation lines initialized, respectively from the same value of δ_D (−79‰) (lower grey line) and the average seasonal δ_D value in regional precipitation (based on Global Network of Isotopes in Precipitation (GNIP) observation).